RESEARCH ARTICLE

Epilepsia®

Atypical intrinsic neural timescales in temporal lobe epilepsy

Ke Xie[1] | Jessica Royer[1] | Sara Lariviere[1] | Raul Rodriguez-Cruces[1] |
Reinder Vos de Wael[1] | Bo-yong Park[1,2,3] | Hans Auer[1] | Shahin Tavakol[1] |
Jordan DeKraker[1] | Chifaou Abdallah[4] | Lorenzo Caciagli[5] | Dani S. Bassett[5,6,7,8,9,10] |
Andrea Bernasconi[11] | Neda Bernasconi[11] | Birgit Frauscher[4] |
Luis Concha[12] | Boris C. Bernhardt[1]

[1]Multimodal Imaging and Connectome Analysis Laboratory, McConnell Brain Imaging Centre, Montreal Neurological Institute, McGill University, Montreal, Quebec, Canada

[2]Department of Data Science, Inha University, Incheon, Republic of Korea

[3]Center for Neuroscience Imaging Research, Institute for Basic Science, Suwon, Republic of Korea

[4]Analytical Neurophysiology Laboratory, Montreal Neurological Institute, McGill University, Montreal, Quebec, Canada

[5]Department of Biomedical Engineering, University of Pennsylvania, Philadelphia, Pennsylvania, USA

[6]Department of Physics and Astronomy, University of Pennsylvania, Philadelphia, Pennsylvania, USA

[7]Department of Electrical and Systems Engineering, University of Pennsylvania, Philadelphia, Pennsylvania, USA

[8]Department of Neurology, University of Pennsylvania, Philadelphia, Pennsylvania, USA

[9]Department of Psychiatry, University of Pennsylvania, Philadelphia, Pennsylvania, USA

[10]Santa Fe Institute, Santa Fe, New Mexico, USA

[11]Neuroimaging of Epilepsy Laboratory, McConnell Brain Imaging Centre, Montreal Neurological Institute, McGill University, Montreal, Quebec, Canada

[12]Brain Connectivity Laboratory, Institute of Neurobiology, Universidad Nacional Autónoma de Mexico (UNAM), Juriquilla, Mexico

Correspondence
Boris C. Bernhardt, McConnell Brain Imaging Centre, Montreal Neurological Institute, Montreal, Quebec H3A 2B4, Canada.
Email: boris.bernhardt@mcgill.ca and boris.bernhardt@gmail.com

Funding information
Canadian Institutes of Health Research; China Scholarship Council, Grant/Award Number: 202006070175; National Research Foundation of Korea, Grant/Award Number: 2021R1F1A1052303; Korea Government (MSIT), Grant/Award Number: 2022-0-00448; Institute for Basic Science, Grant/Award Number: IBS-R015-D1; UNAM-DGAPA

Abstract

Objective: Temporal lobe epilepsy (TLE) is the most common pharmacoresistant epilepsy in adults. Here we profiled local neural function in TLE *in vivo*, building on prior evidence that has identified widespread structural alterations. Using resting-state functional magnetic resonance imaging (rs-fMRI), we mapped the whole-brain intrinsic neural timescales (INT), which reflect temporal hierarchies of neural processing. Parallel analysis of structural and diffusion MRI data examined associations with TLE-related structural compromise. Finally, we evaluated the clinical utility of INT.

Methods: We studied 46 patients with TLE and 44 healthy controls from two independent sites, and mapped INT changes in patients relative to controls across hippocampal, subcortical, and neocortical regions. We examined region-specific associations to structural alterations and explored the effects of age and epilepsy

duration. Supervised machine learning assessed the utility of INT for identifying patients with TLE vs controls and left- vs right-sided seizure onset.

Results: Relative to controls, TLE showed marked INT reductions across multiple regions bilaterally, indexing faster changing resting activity, with strongest effects in the ipsilateral medial and lateral temporal regions, and bilateral sensorimotor cortices as well as thalamus and hippocampus. Findings were similar, albeit with reduced effect sizes, when correcting for structural alterations. INT reductions in TLE increased with advancing disease duration, yet findings differed from the aging effects seen in controls. INT-derived classifiers discriminated patients vs controls (balanced accuracy, 5-fold: 76%±2.65%; cross-site, 72%–83%) and lateralized the focus in TLE (balanced accuracy, 5-fold: 96%±2.10%; cross-site, 95%–97%), with high accuracy and cross-site generalizability. Findings were consistent across both acquisition sites and robust when controlling for motion and several methodological confounds.

Significance: Our findings demonstrate atypical macroscale function in TLE in a topography that extends beyond mesiotemporal epicenters. INT measurements can assist in TLE diagnosis, seizure focus lateralization, and monitoring of disease progression, which emphasizes promising clinical utility.

1 | INTRODUCTION

Temporal lobe epilepsy (TLE) is the most common pharmacoresistant epilepsy in adults. Traditionally considered a "focal" epilepsy with hippocampal pathology as its hallmark, mounting histological and neuroimaging work indicates large-scale reorganization of brain structure.[1] Structural and diffusion magnetic resonance imaging (MRI) studies, in particular, have revealed gray and white matter alterations across multiple cortical and subcortical areas,[1,2] supporting the notion that TLE is a network disorder.[3] Moreover, beyond the identified structural alterations, TLE has long been recognized to also impact brain function.[4,5] A powerful approach to interrogate neural function is the analysis of resting-state functional MRI (rs-fMRI), which offers high spatial resolution and coverage. Prior rs-fMRI studies in TLE have identified atypical functional connectivity within and between temporal and extratemporal regions.[6,7] These are complemented by investigations showing connectome-level reorganization.[8,9] In the literature targeting functional imbalances in TLE, however, notably few studies have characterized intrinsic function at a regional level. In addition to providing a fine-grained mapping of functional alterations, such an approach would allow for targeted assessments of associations between atypical brain structure and function, and would provide regionally precise biomarkers of TLE.

Key points

- Patients with temporal lobe epilepsy (TLE) show shorter intrinsic timescales in multiple regions bilaterally, indexing faster brain activity fluctuations at rest.
- Effects are markedly reduced when correcting for hippocampal atrophy, supporting its central role in whole-brain disease expression.
- Intrinsic neural timescales reductions aggravate with advanced age and disease duration in patients with TLE.
- Intrinsic timescales classify patients vs controls and lateralize TLE with high accuracy and cross-site generalizability.

Beyond the study of spatial variations in functional activity and connectivity, intrinsic functional signaling can also be characterized across temporal scales.[10,11] One marker that has recently emerged from rs-fMRI and electrophysiology work is intrinsic neural timescales (INT), that is, the degree to which spontaneous brain activity correlates with itself over time.[12–14] Long timescales indicate slowly changing activity, whereas short timescales indicate more rapid fluctuations. In healthy individuals, rs-fMRI studies have shown that INT gradually vary along the

sensorimotor-association cortical axis, with shorter INTs in sensory/motor regions and longer INT in medial prefrontal and temporoparietal cortices.[15,16] As such, INTs mirror cortical hierarchies, and could provide a temporal mechanism to organize the integration and segregation of inputs.[14,16] This is also supported by work suggesting spatial similarities in the topography of INT and regional variations of neurostructural properties, including intracortical myelination as well as microcircuit properties.[13,16,17] Because system-level imbalances in connectivity and microcircuit organization have been recognized in TLE,[18,19] measuring alterations in INT would provide a complementary and region-specific viewpoint on brain dysfunctions. Moreover, despite the assumption that brain function is determined largely by underlying structure,[20] there have been only few attempts to consolidate TLE-related changes in local brain function with changes in brain morphology and microstructure. Thus contextualizing INT changes in TLE relative to gray and white matter changes would establish how they occur above and beyond structural perturbations.

Here we mapped the spatial topography of atypical INT in TLE relative to healthy individuals, examined associations to structural alterations, and evaluated clinical utility. Aggregating data from two sites, we opted for a multimodal approach that incorporates rs-fMRI, as well as structural and diffusion MRI in all participants. Our processing paradigm profiled INT alterations at neocortical, subcortical, and hippocampal levels. Further integration of INT findings with markers of gray matter morphology and white matter microstructure evaluated their effects on INT changes. In addition, we explored the correlations between INT and age and epilepsy duration to examine whether dysfunctions in TLE are related to atypical aging and cumulative disease effects. Finally, we assessed how INT parametrization can inform patient vs control classification and seizure focus lateralization using a supervised learning paradigm that implicated cross-validation and inter-site generalization assessments. Multiple sensitivity analyses verified the robustness of our findings.

2 | METHODS

2.1 | Participants

We studied 46 individuals with pharmacoresistant unilateral TLE (18 male; mean ± standard deviation [SD] age = 32.8 ± 12.0 years, 31 left-sided focus) and 44 healthy controls (20 male; mean ± SD age = 32.2 ± 8.6 years) from two imaging sites: (a) *MICA-MICs*, from the Montreal Neurological Institute and Hospital[21]; and (b) *EpiC*, from the Universidad Nacional Autonoma de Mexico.[22] TLE diagnosis and lateralization of seizure foci were determined by criteria of the International League Against Epilepsy (ILAE), based on a comprehensive examination that included clinical history, neurological examination, video-EEG (electroencephalography) recordings, and clinical MRI. Hippocampal atrophy was determined as the absolute hippocampal volumes or interhemispheric asymmetry beyond 2 SD of the corresponding mean of healthy controls[23]: 12 patients (63%) in *MICA-MICs*, and 16 (59%) in *EpiC* had ipsilateral hippocampal atrophy, respectively. As for patients with TLE, we observed no between-site differences in sex (χ^2 = .12, p = .73), the proportion of individuals with a left-/right-sided focus (χ^2 = 1.97, p = .16), and epilepsy duration (t = .35, p = .73). There were differences in age ($t = -2.05$, $p = .05$) and age at onset ($t = -2.95$, $p = .005$). Site-specific demographic and clinical information are provided in Table 1.

TABLE 1 Demographic and clinical characteristics.

	MICA-MICs site			*EpiC* site		
	Controls (n = 23)	TLE (n = 19)	*p*-value	Controls (n = 21)	TLE (n = 27)	*p*-value
Sex, male/female	12/11	8/11	.52[a]	8/13	10/17	.94[a]
Age	34.5 ± 2.9	37.1 ± 11.5	.32[b]	29.8 ± 11.7	29.9 ± 11.5	.98[b]
Seizure focus, L/R	–	15/4	–	–	16/11	–
Age at seizure onset	–	22.0 ± 9.7	–	–	13.4 ± 9.4	–
Disease duration	–	15.1 ± 12.9	–	–	16.5 ± 13.3	–
Hippocampal atrophy[c]	–	12 (63%)	–	–	16 (59%)	–

Note: Age, age at seizure onset, and disease duration are presented in mean ± SD years.

Abbreviations: L, left; R, right; TLE, temporal lobe epilepsy.

[a]chi-square test.

[b]Two-sample *t* test.

[c]Hippocampal atrophy was determined as hippocampal volumes or left–right hippocampal asymmetry beyond 2 SD of the corresponding mean of healthy controls.[23]

2.2 | MRI acquisition and preprocessing

At the *MICA-MICs* site, multimodal data were acquired on a 3T Siemens Magnetom Prisma-Fit. The acquisition included (1) two T1-weighted scans (three-dimensional [3D] magnetization-prepared rapid gradient-echo [MPRAGE], voxel size = $.8 \times .8 \times .8\,mm^3$, matrix size = 320×320, repetition time [TR] = 2300 ms, echo time [TE] = 3.14 ms, flip angle [FA] = 9°, 224 slices); (2) one rs-fMRI scan (multiband accelerated 2D-BOLD echo-planar imaging [EPI], voxel size = $3 \times 3 \times 3\,mm^3$, TR = 600 ms, TE = 30 ms, FA = 52°, field of view [FOV] = $240 \times 240\,mm^2$, multi-band factor = 6, 48 slices, 700 volumes), and (3) one diffusion-MRI scan (2D spin-echo EPI, voxel size = $1.6 \times 1.6 \times 1.6\,mm^3$, TR = 3500 ms, TE = 64.40 ms, FA = 90°, FOV = $224 \times 224\,mm^2$, 3 b0 images). The diffusion-weighted imaging (DWI) consisted of three shells with b-values 300, 700, and $2000\,s/mm^2$, and 10, 40, and 90 diffusion directions per shell, respectively. At the *EpiC* site, multimodal data were acquired on 3T Philips Achieva. The acquisition included (1) one T1-weighted scan (3D spoiled gradient-echo, voxel size = $1 \times 1 \times 1\,mm^3$, TR = 8.1 ms, TE = 3.7 ms, FOV = $179 \times 256 \times 256\,mm^3$, FA = 8°, 240 slices), (2) one rs-fMRI scan (gradient-echo EPI, voxel size = $2 \times 2 \times 3\,mm^3$, TR = 2000 ms, TE = 30 ms, FA = 90°, 34 slices, 200 volumes), and (3) one diffusion-MRI scan (2D EPI, voxel size = $2 \times 2 \times 2\,mm^3$, TR = 11.86 s, TE = 64.3 ms, FOV = $256 \times 256 \times 100\,mm^3$, b-value = $2000\,s/mm^2$, 60 diffusion directions, 2 b0 images). Both sites were preprocessed with *micapipe* (http://micapipe.readthedocs.io/),[24] an open-access processing and data co-registration pipeline. (Full details are described in Supplemental Methods.)

2.3 | Intrinsic neural timescale maps

We estimated INT values at each cortical vertex and in each subcortical region and the hippocampus.[12,25] The autocorrelation function (ACF) of the rs-fMRI timeseries for a given measurement point was calculated using the following formula:

$$ACF_k = \frac{\sum_{t=k+1}^{T}(y_t - \bar{y})(y_{t-k} - \bar{y})}{\sum_{t=1}^{T}(y_t - \bar{y})^2}.$$

For a given region, y denotes the rs-fMRI signal, $\bar{y}$ is the mean signal across timepoints, k is the time lag (time bin = TR), and T is the number of timepoints. Then, INT was calculated as the sum of ACF values in the initial positive period:

$$INT = TR \sum_{k=1}^{N} ACF_k$$

where *TR* is the repetition time of the rs-fMRI signal and *N* is the lag directly preceding the first negative *ACF* value. Multiplying the obtained sum of *ACF* values by *TR* aimed to adjust for differences in the temporal resolution of the rs-fMRI acquisition.[12,25] This procedure was repeated for all vertices, subcortical structures, and hippocampi, generating a whole-brain INT map per participant. Maps in all participants were z-normalized with respect to site-matched controls, followed by sorting patients into ipsilateral/contralateral to the seizure focus.

2.4 | Statistical analysis

2.4.1 | Case–control analysis

As in previous work,[8,26] we fitted surface-based linear models to compare INT values between TLE and controls, controlling for age, sex, and site, using SurfStat[27]:

$$INT_i = \beta_0 + \beta_1 * Age + \beta_2 * Sex + \beta_3 * Site + \beta_4 * Group.$$

For each region *i*, INT_i is the INT score, *Age* and *Sex* are terms controlling for age and sex, respectively. *Site* is the term controlling for the site (i.e., *EpiC*, *MICA-MICs*) and *Group* is the group factor (i.e., TLE, controls). We separately evaluated the consistency of findings in each site, repeating the above comparisons while controlling for age and sex:

$$INT_i = \beta_0 + \beta_1 * Age + \beta_2 * Sex + \beta_3 * Group.$$

As seizure focus lateralization may differentially affect the spatial topography of atypical INT, we repeated the above analyses in the left ($n_{LTLE} = 31$) and right ($n_{RTLE} = 15$) TLE separately, comparing both subgroups to controls.

2.4.2 | Control for morphology and microstructure

To assess INT changes above and beyond morphological and microstructural changes, we examined case–control INT differences while additionally correcting for vertex-wise cortical thickness or diffusion features.[8,28] For subcortical structures and the hippocampus, we controlled for the corresponding volume and average diffusion parameters in the surrounding shell.[18,26]

2.4.3 | Age and disease duration effects

We first built linear models that included an *age* and *group* main effect term, and an age × group interaction

term. We separately evaluated the effects of age on INT in each group. To probe cumulative disease factors in TLE, we assessed the effects of epilepsy duration and age at seizure onset.

$$INT_i = \beta_0 + \beta_1 * Age + \beta_2 * Sex + \beta_3 * Site$$
$$+ \beta_4 * Group + \beta_5 * (Age \times Group)$$

2.4.4 | Sensitivity analyses

Several analyses verified robustness. First, we repeated the case–control INT analysis while controlling for head motion, after calculating individualized mean framewise displacement (FD) during the rs-fMRI scan.[29] We also repeated the INT comparisons while additionally regressing out various confounding features of rs-fMRI processing, including global mean signal and temporal signal-to-noise ratio (tSNR)

2.4.5 | Correction for multiple comparisons

Findings were corrected by controlling the family-wise error (FWE) at $p_{FWE} < .05$ for neocortex, and false discovery rate (FDR) at $p_{FDR} < .05$ for subcortical structures and the hippocampus, respectively.

2.5 | Spatial permutation tests

To assess the consistency of findings across sites, we statistically compared the patterns of case–control INT differences. In the neocortex, the statistical significance of spatial correlations was assessed using 1000 spin permutation tests, implemented in BrainSpace.[30] This framework generated null models of similarity between two given cortical maps, by projecting the spatial coordinates of cortical data onto the surface spheres, applying randomly sampled rotations, and reassigning each vertex with the value of its nearest neighbors. The originally observed correlation coefficient of two spatial maps was placed in the null distribution of rotated correlation coefficients (associated p-values are denoted p_{spin}). A similar framework evaluated the correspondence between subcortical maps, with the exception that subcortical labels were shuffled randomly while preserving pairwise Euclidean distances (associated p-values are denoted p_{shuf}),[31,32] using the ENIGMA Toolbox.[33]

2.6 | Classification and lateralization analysis

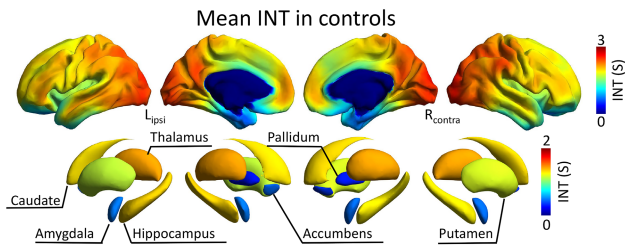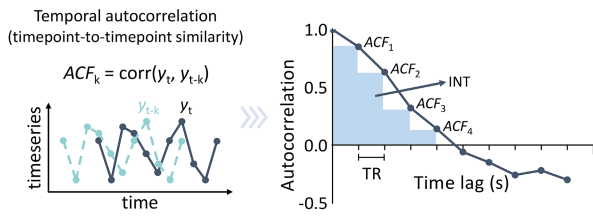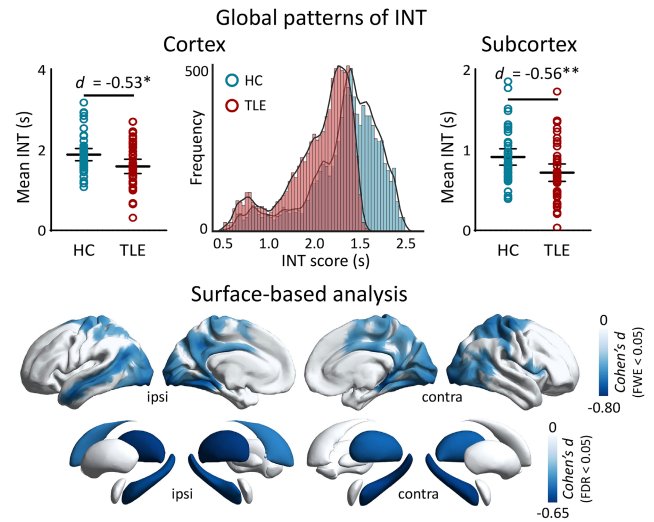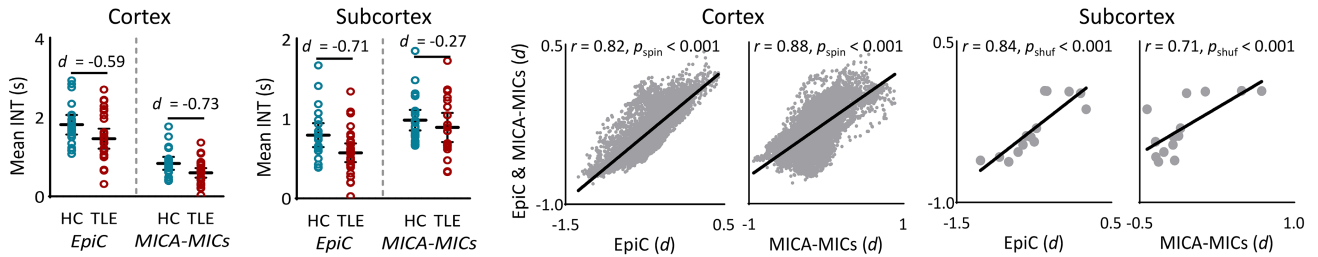We utilized support vector machines, implemented in LIBSVM,[34] to examine how well INT can discriminate TLE patients from controls, and lateralize patients. Two models were evaluated: (1) neocortical features only and (2) neocortical, subcortical, and hippocampal features (for further details, see Supplemental Methods). Models were validated in two scenarios. First, classifiers were trained and tested across two sites using 5-fold cross-validation with 100 iterations. The statistical significance was evaluated using 1000 permutation tests thresholded at $p < .05$. Second, we assessed cross-site generalizability, where classifiers were trained on one site with leave-one-out cross-validation and tested on the other site. Performance was assessed using balanced accuracy (BACC) and area under the curve (AUC) of the receiver-operating characteristic (ROC) curves. In addition, to assess whether INT can improve the TLE-vs-controls discrimination, and left-vs-right TLE lateralization, we benchmarked our model performance against a baseline model based on structural MRI-derived parameters (features included cortical thickness and subcortical volume). Performance of models was compared directly using McNemar's tests.

3 | RESULTS

3.1 | Group differences in INT

In controls, we observed relatively long INT in parieto-occipital cortices, but shorter INT in sensorimotor and temporolimbic cortices. In other words, higher-order association areas showed slower processing timescales compared to sensorimotor areas with faster signal fluctuations.[13,15] Subcortically, longer INT were seen in the thalamus, and shorter INT in the amygdala, nucleus accumbens, and pallidum (Figure 1A and Appendix S1).

Globally, neocortical, subcortical, and hippocampal INT values were reduced in TLE (neocortex: *Cohen's d* = −.53, $p < .05$; subcortex and hippocampus: $d = -.56$, $p < .01$; Figure 1B). Surface-wide analysis revealed INT reductions in TLE in the bilateral precuneus, parietal and occipital cortices, and the ipsilateral temporal lobe ($p_{FWE} < .05$; mean effect sizes in significant clusters: d [mean ± SD] = −.48 ± .09), along with bilateral hippocampus and thalamus ($p_{FDR} < .05$; $d = -.56 ± .07$; Figure 1B). That is, patients with TLE exhibited faster activity fluctuations in these regions than controls. As seizure focus laterality may differentially impact the patterns of atypical INT, we repeated the surface-based INT analyses by comparing left and right TLE separately from controls. Common patterns of INT reductions involving the ipsilateral middle temporal gyrus, and bilateral occipital cortex, parahippocampal gyrus ($p_{FWE} < .05$), and hippocampus ($p_{FDR} < .085$) were found in both TLE cohorts (Figure S3). Left TLE additionally showed atypical INT in

FIGURE 1 Intrinsic neural timescales (INT) reductions in temporal lobe epilepsy (TLE). (A) Calculation of INT from resting-state functional magnetic resonance imaging (rs-fMRI) data. INT is defined as the sum of timepoint-to-timepoint autocorrelation function (ACF) values in the initial positive period (i.e., the sum of the area of blue bars) and multiplied by the repetition time (TR).[12,25] Example plots of empirical ACF values for rs-fMRI data of *EpiC* site where TR = 2 s. Surface-wide maps in the *bottom* panel show the group-averaged, whole-brain INT values in healthy controls. (B) Differences in INT between TLE and controls, controlling for age, sex, and site. *Top*: Global mean and distributions of regional INT. *Bottom*: INT reductions in TLE relative to controls after correcting for multiple comparisons at a family-wise error (FWE) rate < .05 for neocortex, and at a false discovery rate (FDR) < .05 for subcortex and the hippocampus. (C) Cross-site consistency. *Left*: Group differences in global mean INT in each site separately. Each circle represents each individual's global mean INT. *Right*: Associations of *Cohen's d* value from site-pooled data (i.e., *EpiC* & *MICA-MICs*; y-axis) and *Cohen's d* from each site independently. Each dot indicates a vertex or subcortical structure. The statistical significance of spatial correlations is determined using 1000 permutation tests (associated *p*-values are denoted p_{spin} for neocortex, and p_{shuf} for subcortex and hippocampus).[31] HC, healthy control; TLE, temporal lobe epilepsy; ipsi, ipsilateral; contra, contralateral. *$p < .05$; **$p < .01$.

the bilateral precuneus and contralateral superior parietal lobe ($p_{FWE} < .05$), whereas right TLE additionally showed alterations in the ipsilateral insula ($p_{FWE} < .05$), bilateral thalamus (left/right $p_{FDR} = .053/.006$), caudate nucleus (left/right $p_{FDR} = .066/.053$), and putamen (left/right $p_{FDR} = .078/.053$).

Findings were consistent across sites, albeit with subtle differences in effect sizes (*EpiC*: neocortex, $d = -.59$; subcortex and hippocampus, $d = -.73$; *MICA-MICs* = $-.36/-.27$; Figure 1C and Figure S2). Site-pooled effect sizes also showed high spatial similarity to those from single sites (*EpiC*: neocortex, $r = .82$, $p_{spin} < .001$; subcortex and hippocampus, $r = .84$, $p_{shuf} < .001$; *MICA-MICs*: $r = .88/.71$, $p_{spin}/p_{shuf} < .001$).

Results were robust with respect to head motion and other image processing parameters. Specifically, between-group

differences in INT were virtually identical when controlling for participant-specific mean FD (neocortex: $r = .95$, $p_{spin} < .001$, $d = -.51 \pm .08$; subcortex and hippocampus: $r = .91$, $p_{shuf} < .001$, $d = -.60 \pm .07$; Figure S4). Repeat analyses that additionally included the global mean signal as covariates, revealed a virtually identical spatial distribution of INT reductions (neocortex: $r = .76$, $p_{spin} < .001$; subcortex and hippocampus: $r = .88$, $p_{shuf} = .003$; Figure S4). Note that, however, global mean signal correction reduced subcortical and hippocampal effects ($d = -.46 \pm .05$). Finally, we repeated the INT comparisons after adding vertex-wise tSNR as a covariate of non-interest in surface-based linear models, and observed virtually identical effects ($r = .98$, $p_{spin} < .001$, $d = -.49 \pm .09$; Figure S5), suggesting no strong influence of inter-regional variations in tSNR.

3.2 | Effects of cortical morphology and microstructure

Compared to controls, patients with temporal lobe epilepsy (TLE) showed cortical thinning in the bilateral paracentral, dorsomedial, and ventromedial prefrontal regions ($p_{FWE} < .05$) as well as the ipsilateral hippocampus ($p_{FDR} < .05$) (Figure 2A), confirming prior findings.[3,26] After controlling for gray matter variations, we observed virtually identical spatial patterns of INT changes (neocortex: $r = .99$, $p_{spin} < .001$; subcortex and hippocampus: $r = .93$, $p_{shuf} < .001$; Figure 2A), and effect sizes in regions of significant neocortical INT reductions (see Figure 1B) were comparable ($d = -.47 \pm .09$, 2% reduction). However, the extent of subcortical and hippocampal INT changes was more markedly reduced ($d = -.47 \pm .10$, 16% reduction) when correcting for corresponding volume, specifically in the ipsilateral hippocampus (48% reduction; Figure S6).

In addition, we replicated earlier findings by showing superficial microstructural alternations in TLE, characterized by reduced FA and increased MD (Figure S7), in the ipsilateral temporolimbic cortices ($p_{FWE} < .05$) and in areas surrounding the bilateral hippocampi and thalamus ($p_{FDR} < .05$; Figure 2B).[8,18,28] INT group differences were similar albeit slightly weaker in models that additionally controlled for these metrics (neocortex: $r = .95$, $p_{spin} < .001$, $d = -.46 \pm .09$, 4% reduction; subcortex and hippocampus: $r = .99$, $p_{shuf} < .001$, $d = -.48 \pm .09$, 14% reduction; Figure S6). Furthermore, correcting for both morphological and microstructural metrics also
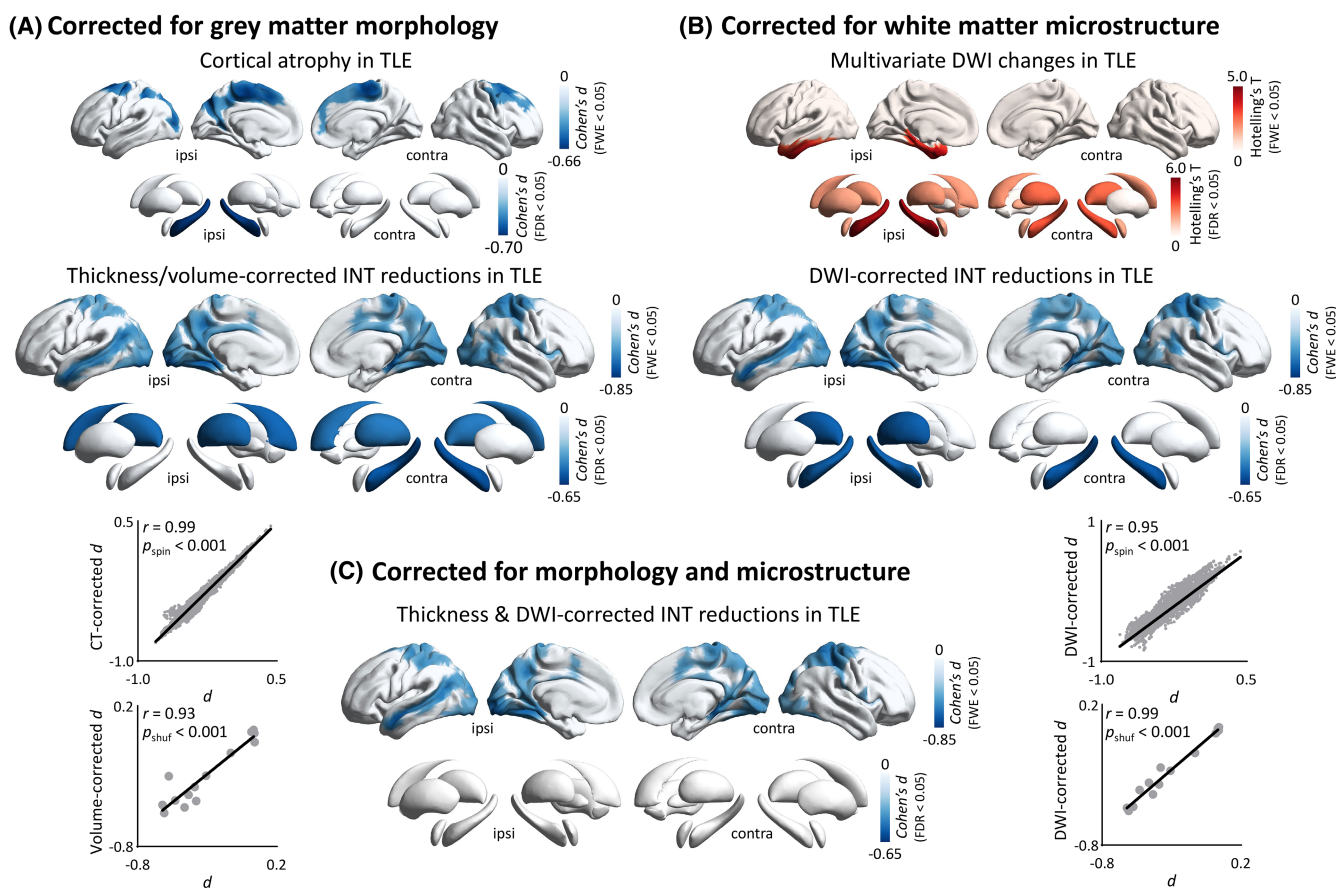
FIGURE 2 Effects of cortical structural perturbations on intrinsic neural timescales (INT) reductions. (A) Regional cortical thickness and subcortical volume changes in temporal lobe epilepsy (TLE) compared to controls. INT reductions were similar after controlling for cortical thickness. Similar findings were seen for subcortical structures and the hippocampus. Scatterplots of *Cohen's d* values from original INT reductions (x-axis; see Figure 1B) vs thickness-/volume-corrected INT reductions (y-axis). (B) Multivariate superficial white matter changes in TLE relative to controls. INT reductions remained robust when controlling for diffusion effects at each vertex or surrounding subcortical structures and the hippocampus. Scatterplots of *Cohen's d* values from original INT reductions (x-axis; see Figure 1B) vs diffusion-weighted imaging (DWI)–corrected INT reductions (y-axis). The significance of spatial correlations was determined using 1000 permutation tests (associated p-values are denoted p_{spin} for neocortex, and p_{shuf} for subcortex and hippocampus).[31] (C) INT reductions in TLE relative to controls after additionally controlling for both gray matter morphological and white matter microstructural measures. Findings had been corrected for multiple comparisons (See Figure 1 for details). TLE, temporal lobe epilepsy; ipsi, ipsilateral; contra, contralateral; CT, cortical thickness.

did not modify the spatial distributions of INT changes (Figure 2C; neocortex, $r = .99$, $p_{spin} < .001$; subcortex and hippocampus, $r = .93$, $p_{shuf} < .001$), but reduced the effect sizes (neocortex, $d = -.45 \pm .09$, 6% reduction; subcortex, $d = -.41 \pm .02$, 22% reduction; ipsilateral hippocampus, $d = -.39$, 32% reduction; Figure S6), with only the neocortex showing significant INT reductions in TLE.

3.3 | Effects of age and disease duration on INT

Globally, we observed significant correlations between age and mean cortical and subcortical INT in TLE after controlling for sex and site ($r = -.33/-.33$, $p = .027/.025$; Figure 3A), but not in controls ($r = .12/-.10$, $p = .464/.505$). Moreover, there was a significant discrepancy in cortical slopes between TLE and controls (t-value $= -2.12$, $p = .017$), supporting that the relationship between INT reductions and aging in TLE differed from controls. Surface-wide age × group interactions confirmed the above findings and pointed to significant findings in the bilateral sensorimotor and occipital regions and the ipsilateral temporal lobe ($p_{FWE} < .05$; Figure 3A). Post hoc analyses showed that INT increased in these regions in controls with advancing age, whereas the inverse was observed in TLE (Figure 3A,B). When analyses were repeated separately in *EpiC* and *MICA-MICs*, age-related negative effects in TLE were observed in almost all brain

regions in each site and patterns resembled those derived from site-pooled data (Figure S8). That is, across-site differences in data acquisition protocols (e.g., repetition time) and demographic variables (e.g., age) did not affect our findings considerably. Moreover, INT negatively correlated with epilepsy duration, with prominent effects in the bilateral temporal and prefrontal regions, and the ipsilateral precuneus and paracentral regions ($p_{FWE} < .05$). There was a trend toward significance for the negative effects of epilepsy duration on subcortical INT, particularly in bilateral thalamus (Figure S9; $p_{FDR} < .075$). There were no significant main effects of age at seizure onset on INT ($p_{FWE}/p_{FDR} < .05$).
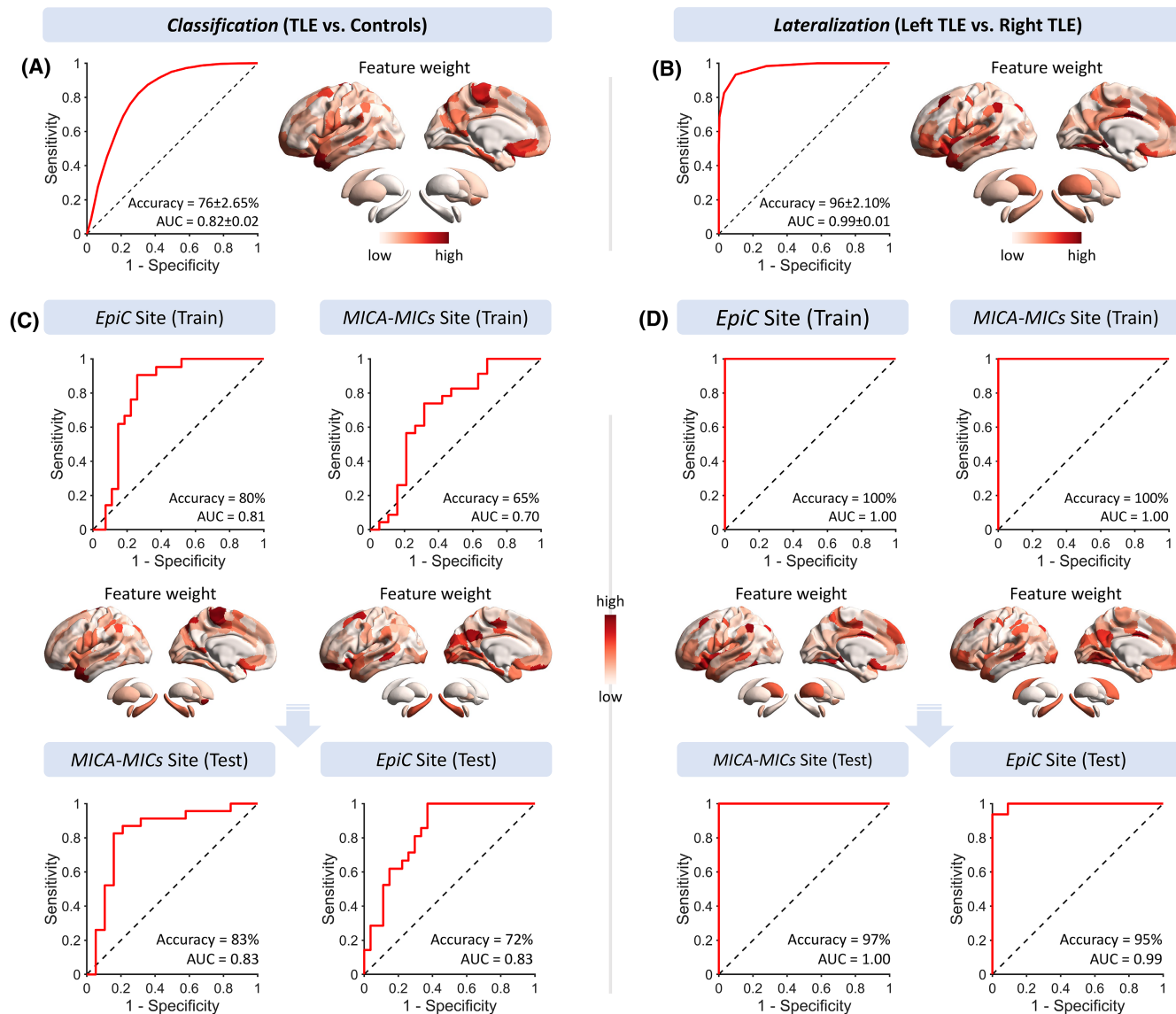
3.4 | Classification and lateralization performance

Using supervised statistical learning, we examined how well INT can discriminate patients from controls and lateralize the seizure focus in TLE. In the classification analyses, the combination of cortical and subcortical INT achieved a balanced accuracy of $76 \pm 2.65\%$ ($p = .001$) and AUC of $.82 \pm .02$ ($p = .001$) (Figure 4A and Table 2). Selected features mapped onto the temporal pole, parahippocampal gyrus, and medial orbitofrontal and paracentral cortices (Figure 4A). In the lateralization analysis, the overall balanced accuracy was $96 \pm 2.10\%$ ($p = .001$) and the AUC was $.99 \pm .01$ ($p = .001$), based on the combination
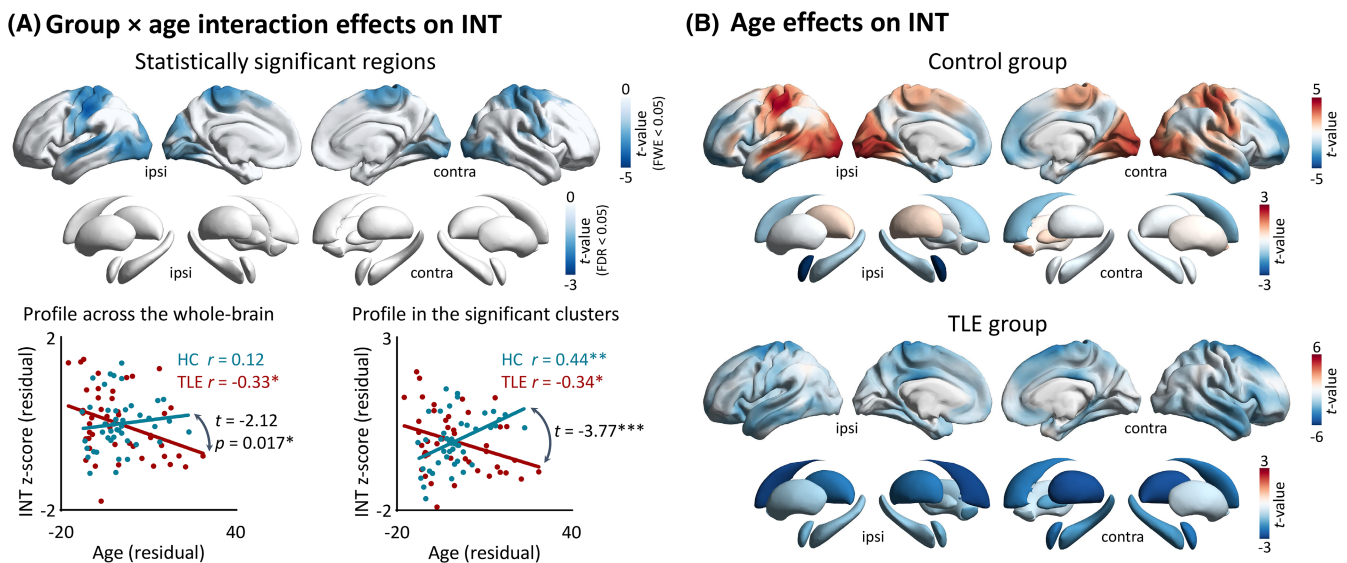
FIGURE 3 Effects of age on intrinsic neural timescales (INT). (A) Interaction between age and group. *Top*: Regions showing a more pronounced, negative effect of age on INT in temporal lobe epilepsy (TLE) after multiple comparisons correction (see Figure 1 for details). *Bottom*: Correlations between age and mean INT of the entire neocortex (*left*) and the regions with significant age × group interaction effects (*right*) in each group separately. (B) Main effects of age on INT in controls and the TLE group independently, with INT increasing/decreasing as aging shown in red/blue. HC, healthy controls; TLE, temporal lobe epilepsy; ipsi, ipsilateral; contra, contralateral. *$p < .05$; **$p < .01$; ***$p < .001$.

FIGURE 4 Classification and lateralization analyses based on cortical and subcortical intrinsic neural timescales (INT). Support vector machines are used to classify temporal lobe epilepsy (TLE) vs controls (*left*) and left vs right TLE (*right*). (A) and (B) Performance of classifiers trained and tested on site-pooled data, using 5-fold cross-validation. Average receiver-operating characteristic (ROC) curves, normalized feature weight maps, balanced accuracy, and area under curve (AUC, mean ± SD) across 100 iterations are indicated. (C) and (D) Performance of classifiers trained on one site using leave-one-out cross-validation and tested on the other one.

TABLE 2 Classification and lateralization performance using combined cortical and subcortical features.

	EpiC & MICA-MICs		EpiC (train) → MICA-MICs (test)				MICA-MICs (train) → EpiC (test)			
	BACC[a]	AUC[a]	BACC	AUC	BACC	AUC	BACC	AUC	BACC	AUC
Classification	76 ± 2.65%	.82 ± .02	80%	.81	83%	.83	65%	.70	72%	.83
Lateralization	96 ± 2.10%	.99 ± .01	100%	1.00	97%	1.00	100%	1.00	95%	.99

Abbreviations: AUC, area under curve; BACC, balanced accuracy.

[a]BACC and AUC in mean ± SD.

of cortical and subcortical INT. Informative features were found in the paralimbic cortex, encompassing the temporal pole and insula (Figure 4B). Models generalized well from one site to another one (Figure 4C,D, Table 2). Notably, models based on only cortical INT showed comparable performance (Figure S10 and Table S1).

Moreover, our models based on INT features performed significantly better (McNemar's tests, all $p < .001$) than a baseline model that used structural MRI-derived features in both classification (cortical thickness and subcortical volume: accuracy/AUC, $65 \pm 3.68\%/.67 \pm .04$; cortical thickness alone, $64 \pm 3.00\%/.66 \pm .04$) and lateralization ($52 \pm 3.48\%/.76 \pm .20$; $51 \pm 3.01\%/.76 \pm .19$; Figure S11).

4 | DISCUSSION

The current work set out to (1) map the topography of atypical intrinsic neural timescales (or INT) in TLE relative to controls, (2) examine the associations with morphological and microstructural perturbations, and (3) assess whether INT changes are sensitive to cumulative disease effects and accurate markers for automated patient-vs-control classification and seizure-focus lateralization. Studying a two-site dataset of TLE and controls, we observed widespread INT reductions in TLE, with marked effects in temporolimbic and sensorimotor areas, as well as the thalamus and hippocampus. Results remained consistent, albeit of smaller effect sizes, after controlling for structural variations. Furthermore, correlation analyses with age and disease duration revealed that INT effects aggravated with advanced age and disease duration in TLE, a finding supportive of progressive alterations in intrinsic brain function. Finally, INT-informed supervised classifiers classified patients vs controls, and lateralized the seizure focus with high accuracy and cross-site generalizability. Collectively, our findings outline extensive intrinsic functional imbalances in TLE, which may advance our understanding of structure–function relationships and the development of functional imaging biomarkers in the condition.

Core to our work was the quantification of INT using rs-fMRI data, a recently developed measure that taps into the temporal autocorrelation of neural signals.[13,15] In our controls, this measure differentiated sensorimotor systems from heteromodal association cortices with longer timescales, in agreement with prior work in healthy adults[13,15,16] and developing neurotypical cohorts.[12] Differences in timescales have been related previously to the functional hierarchy of the human cortex.[13] In particular, shorter INT in sensorimotor systems have been associated with their more specialized, externally oriented functional roles, implicated in facilitating neural responsiveness to changing environmental contexts. On the other hand, longer INT in heteromodal regions may contribute to their role in multisensory integration as well as abstract, higher-order processing.[13,16] In typical development, prior studies have shown changes in INT with aging, in particular a lengthening of neural timescales in heteromodal

and paralimbic cortices,[35] which parallels the ongoing microstructural and connectional differentiation in these regions throughout childhood and adolescence.[36] To identify regional patterns of functional imbalances in TLE, we fitted neocortical, hippocampal, and subcortical models that additionally controlled for the effects of age, sex, and site. This provided robust evidence for widespread INT reductions in TLE, in a cortical–subcortical territory encompassing the hippocampus and thalamus, alongside lateral temporal, parieto-occipital, and paracentral regions.[3] Effects appeared bilateral yet more extensive ipsilaterally. This was particularly seen in temporal regions, where INT extended anteriorly to temporopolar cortices. Despite some differences in effect sizes, patterns of reduced INT in TLE were replicable across independently acquired datasets, thus being robust to cross-site differences in acquisition protocols and some in clinical and sociodemographic inclusion. It is of note that altered INT patterns in TLE were preserved when additionally controlling for participant-specific head motion and inter-regional variations in tSNR. Moreover, results were broadly similar albeit slightly weaker in the subcortex and hippocampus when additionally regressing out the global mean signal. These, therefore, confirm that our main findings are not related to spurious features.

Prior rs-fMRI studies examined inter-regional connectivity in TLE, and showed atypical functional interactions within and between mesiotemporal and extra-temporal.[5–7] In addition, some works suggest alterations in signal amplitude[28] or regional signaling homogeneity of neural signals.[37] By robustly demonstrating TLE-related INT reductions across a broad neocortical, hippocampal, and subcortical territory, our work expands this literature by identifying a functional signature characterized by changes in the spatial and temporal domain. Temporal lobe structures, in particular the mesiotemporal region, as well as the thalamus have long been recognized as critical nodes in the TLE network. Prior research based on intracranial electroencephalography explorations in human patients and animal models has supported that the hippocampus and adjacent mesiotemporal as well temporopolar regions are highly epileptogenic. Moreover, these regions together with thalamocortical loops play a crucial role in the propagation of both inter-ictal spiking activity to more distributed cortical networks.[18] In the absence of parallel explorations of electrical activity in the same patients, we cannot confidently say how INT changes ultimately predispose brain networks to transient epileptic phenomena. Yet, it is tempting to speculate that the overall reduction in INT across multiple key nodes in the TLE network may reflect a chronic functional imbalance that may more likely generate epileptic phenomena in its dynamic regime. By combining transcriptomics with in vivo

functional imaging in healthy individuals, recent work has shown a direct alignment between INT and expression of excitation- and inhibition-related genes,[13] which may suggest relations to the local excitation–inhibition ratio.[13,17] Our group recently leveraged connectome-informed brain models in TLE, and also identified distributed patterns of cortical E/I imbalances, together with reductions in subcortical drive.[18] Despite limited data on the interaction between these chronic alterations in intrinsic brain function and transient epileptic events, it is plausible that a chronic functional imbalance, as indicated by reduced INT, may also predispose brain networks to exhibit transient epileptic states.[38] An earlier study reported state-dependent changes in global network dynamics, as indicated by a decrease of neuronal synchronization during seizures and increases prior to seizure termination,[4] consistent with the above conjecture.

Structural and diffusion MRI studies in TLE have previously mapped patterns of cortical and subcortical morphological changes as well as atypical fiber diffusivity in deep and superficial white matter. Capitalizing on an advanced multimodal MRI processing and feature fusion framework,[24] we examined associations between INT changes and co-occurring structural perturbations in the same participants. Patterns of gray matter atrophy and white matter diffusion alterations observed in the current work confirmed prior studies, suggesting bilateral cortico-subcortical atrophy and a predominance of temporolimbic changes in superficial white matter microstructure.[8,18,28] Notably, although the spatial patterns of INT reductions in TLE were similar after correcting for both gray and white matter changes, the effect sizes of INT changes decreased, particularly in the hippocampus. These suggest, on the one hand, that INT changes provide unique information that is not comprehensively explained by alterations in cortical morphology and microstructure; on the other hand, there exists nonetheless shared variance between structural and functional alterations. Marked modulations of functional matrices by structural features, as observed in the mesiotemporal lobe, also highlighted the role of the hippocampus as TLE pathological core.[3,39] As such, these findings provide a system-level functional complement to previous work showing marked modulatory effects of hippocampal pathology on large-scale white matter network topology and connectome-informed network communication models.[8,39]

Performing an age-by-group interaction analysis provided a cross-sectional window into potentially progressive functional changes in TLE, and their differences from typical aging effects seen in controls.[3] Specifically, we found more negative effects of age in patients with TLE than in controls in bilateral primary cortices and ipsilateral temporal regions. Patterns in TLE were also significantly associated with disease duration, which may indicate multiple parallel processes, notably the cumulative effects of ongoing seizures. Site-specific findings were comparable when repeating analyses in each of our two sites separately, suggesting rather marginal influences of cross-site differences in MRI acquisition parameters and demographic as well as clinical characteristics. Despite an incompletely understood association between seizures and local function, seizure-related brain re-organization has been supported by studies using animal models of limbic epilepsy.[40] Moreover, MR spectroscopic work in TLE has suggested associations of seizure burden and neural integrity,[41] and there is relatively convincing evidence from cross-sectional and longitudinal analyses of gray matter morphology indicating progressive atrophy in TLE.[26,42] On the other hand, except for prior research showing progressive effects on *in vivo* PET-derived glucose metabolism data,[43] findings demonstrating age-related effects on intrinsic function at the whole-brain level in TLE have remained scarce until now. Our study thus provides a potential region-specific functional complement to the extant structural literature. Arguably, and beyond seizure-related effects, our findings showing more marked INT reductions in TLE with advanced aging and duration may also signify the effects of continued treatment with antiseizure medication.[38] Accelerated aging processes in INT observed here also are in line with observations of vascular alterations in TLE[44] and emerging histopathological reports, suggesting a higher presence of neurodegenerative deposits, including misfolded tau protein, in surgical tissue resected from TLE.[45] Future work tracking changes in brain function and structure longitudinally, alongside careful monitoring of clinical and cognitive phenotypes, will help further sharpen our understanding of causes and consequences of epilepsy-associated progression. To account for a likely broad range of susceptibility and resilience factors across patients, such efforts would certainly benefit from multi-site datasets like ENIGMA-Epilepsy.[46]

Leveraging supervised machine learning, we demonstrated that classifiers informed by INT could discriminate TLE from controls and lateralize seizure focus with high accuracy. These findings complement earlier efforts in epilepsy classification and focus lateralization using a wide range of features from structural MRI, diffusion MRI, and rs-fMRI functional connectivity analysis.[47,48] We further specifically assessed cross-site prediction and confirmed adequate inter-site generalization performance, contrasting most of the existing work that evaluated classifiers using single-site data. Another advance offered by the present study is that we provided valuable information about brain regions contributing highly to classifiers, thus enhancing our biological understanding of diagnostic imaging markers. Informative features included

mesiotemporal areas, but also spanned beyond these, likely reflecting the known system-level involvement of TLE. Highlighting a promising clinical utility of INT for personalized diagnostics in TLE, our findings motivate the development of a unified technique that combines a wide scope of structural and connectional measures with biologically meaningful indices of neural function, such as INT.

AUTHOR CONTRIBUTIONS

ACKNOWLEDGMENTS

CONFLICT OF INTEREST STATEMENT

None of the authors has any conflict of interest to disclose.

PATIENT CONSENT STATEMENT

The study has been approved by the Research Ethics Boards of the Montreal Neurological Institute and Hospital and the Universidad Nacional Autónoma de Mexico, respectively. Written informed consent was obtained from all participants in accordance with the Declaration of Helsinki.

CODE AVAILABILITY

The pipeline used for MRI data pre-processing is openly available at https://github.com/MICA-MNI/micapipe and http://micapipe.readthedocs.io. The SurfStat toolbox used for surface-based statistical analysis is available at http://math.mcgill.ca/keith/surfstat/ or https://mica-mni.github.io/surfstat/. The LIBSVM toolbox used for machine learning is available at https://www.csie.ntu.edu.tw/~cjlin/libsvm/index.html. Code used for the main analyses is available at http://github.com/MICA-MNI/micaopen/. Surface-based INT features are available at https://osf.io/m4fap/.

ORCID

Jessica Royer https://orcid.org/0000-0002-4448-8998
Sara Lariviere https://orcid.org/0000-0001-5701-1307
Andrea Bernasconi https://orcid.org/0000-0001-9358-5703
Neda Bernasconi https://orcid.org/0000-0002-8947-9518
Birgit Frauscher https://orcid.org/0000-0001-6064-1529
Luis Concha https://orcid.org/0000-0002-7842-3869
Boris C. Bernhardt https://orcid.org/0000-0001-9256-6041

REFERENCES

1. Whelan CD, Altmann A, Botia JA, Jahanshad N, Hibar DP, Absil J, et al. Structural brain abnormalities in the common epilepsies assessed in a worldwide ENIGMA study. Brain. 2018;141(2):391–408.
2. Hatton SN, Huynh KH, Bonilha L, Abela E, Alhusaini S, Altmann A, et al. White matter abnormalities across different epilepsy syndromes in adults: an ENIGMA-epilepsy study. Brain. 2020;143(8):2454–73.
3. Lariviere S, Rodríguez-Cruces R, Royer J, Caligiuri ME, Gambardella A, Concha L, et al. Network-based atrophy modeling in the common epilepsies: a worldwide ENIGMA study. Sci Adv. 2020;6(47):eabc6457.
4. Schindler KA, Bialonski S, Horstmann M-T, Elger CE, Lehnertz K. Evolving functional network properties and

synchronizability during human epileptic seizures. Chaos. 2008;18(3):33119.

5. Pereira FRS, Alessio A, Sercheli MS, Pedro T, Bilevicius E, Rondina JM, et al. Asymmetrical hippocampal connectivity in mesial temporal lobe epilepsy: evidence from resting state fMRI. BMC Neurosci. 2010;11(1):66.

6. Bernhardt BC, Bernasconi A, Liu M, Hong S-J, Caldairou B, Goubran M, et al. The spectrum of structural and functional imaging abnormalities in temporal lobe epilepsy. Ann Neurol. 2016;80(1):142–53.

7. Li H, Ding F, Chen C, Huang P, Xu J, Chen Z, et al. Dynamic functional connectivity in modular organization of the hippocampal network marks memory phenotypes in temporal lobe epilepsy. Hum Brain Mapp. 2021;43(6):1917–29.

8. Lariviere S, Weng Y, Vos de Wael R, Royer J, Frauscher B, Wang Z, et al. Functional connectome contractions in temporal lobe epilepsy: microstructural underpinnings and predictors of surgical outcome. Epilepsia. 2020;61(6):1221–33.

9. Yang S, Zhang Z, Chen H, Meng Y, Li J, Li Z, et al. Temporal variability profiling of the default mode across epilepsy subtypes. Epilepsia. 2021;62(1):61–73.

10. Maturana MI, Meisel C, Dell K, Karoly PJ, D'Souza W, Grayden DB, et al. Critical slowing down as a biomarker for seizure susceptibility. Nat Commun. 2020;11(1):2172.

11. Scheid BH, Ashourvan A, Stiso J, Davis KA, Mikhail F, Pasqualetti F, et al. Time-evolving controllability of effective connectivity networks during seizure progression. Proc Natl Acad Sci U S A. 2021;118(5):e2006436118.

12. Watanabe T, Rees G, Masuda N. Atypical intrinsic neural timescale in autism. Elife. 2019;8:e42256.

13. Gao R, van den Brink RL, Pfeffer T, Voytek B. Neuronal timescales are functionally dynamic and shaped by cortical microarchitecture. Elife. 2020;9:e61277.

14. Wolff A, Berberian N, Golesorkhi M, Gomez-Pilar J, Zilio F, Northoff G. Intrinsic neural timescales: temporal integration and segregation. Trends Cogn Sci. 2022;26(2):159–73.

15. Raut RV, Snyder AZ, Raichle ME. Hierarchical dynamics as a macroscopic organizing principle of the human brain. Proc Natl Acad Sci U S A. 2020;117(34):20890–7.

16. Ito T, Hearne LJ, Cole MW. A cortical hierarchy of localized and distributed processes revealed via dissociation of task activations, connectivity changes, and intrinsic timescales. Neuroimage. 2020;221:117141.

17. Li S, Wang X-J. Hierarchical timescales in the neocortex: mathematical mechanism and biological insights. Proc Natl Acad Sci U S A. 2022;119(6):e2110274119.

18. Weng Y, Lariviere S, Caciagli L, Vos de Wael R, Rodriguez-Cruces R, Royer J, et al. Macroscale and microcircuit dissociation of focal and generalized human epilepsies. Commun Biol. 2020;3(1):244.

19. Fadaie F, Lee HM, Caldairou B, Gill RS, Sziklas V, Crane J, et al. Atypical functional connectome hierarchy impacts cognition in temporal lobe epilepsy. Epilepsia. 2021;62(11):2589–603.

20. Suárez LE, Markello RD, Betzel RF, Misic B. Linking structure and function in macroscale brain networks. Trends Cogn Sci. 2020;24(4):302–15.

21. Royer J, Rodríguez-Cruces R, Tavakol S, Lariviere S, Herholz P, Li Q, et al. An open MRI dataset for multiscale neuroscience. Sci Data. 2022;9(1):569.

22. Rodriguez-Cruces R, Bernhardt BC, Concha L. Multidimensional associations between cognition and connectome organization in temporal lobe epilepsy. Neuroimage. 2020;213:116706.

23. Bernasconi N, Bernasconi A, Caramanos Z, Antel SB, Andermann F, Arnold DL. Mesial temporal damage in temporal lobe epilepsy: a volumetric MRI study of the hippocampus, amygdala and parahippocampal region. Brain. 2003;126(Pt 2):462–9.

24. Cruces RR, Royer J, Herholz P, Lariviere S, de Wael RV, Paquola C, et al. Micapipe: a pipeline for multimodal neuroimaging and connectome analysis. Neuroimage. 2022;263:119612.

25. Wengler K, Goldberg AT, Chahine G, Horga G. Distinct hierarchical alterations of intrinsic neural timescales account for different manifestations of psychosis. Elife. 2020;9:e56151.

26. Bernhardt BC, Bernasconi N, Concha L, Bernasconi A. Cortical thickness analysis in temporal lobe epilepsy: reproducibility and relation to outcome. Neurology. 2010;74(22):1776–84.

27. Worsley KJ, Taylor JE, Carbonell F, Chung MK, Duerden E, Bernhardt B, et al. SurfStat: a Matlab toolbox for the statistical analysis of univariate and multivariate surface and volumetric data using linear mixed effects models and random field theory. Neuroimage. 2009;47:S102.

28. Liu M, Bernhardt BC, Hong SJ, Caldairou B, Bernasconi A, Bernasconi N. The superficial white matter in temporal lobe epilepsy: a key link between structural and functional network disruptions. Brain. 2016;139(Pt 9):2431–40.

29. Power JD, Mitra A, Laumann TO, Snyder AZ, Schlaggar BL, Petersen SE. Methods to detect, characterize, and remove motion artifact in resting state fMRI. Neuroimage. 2014;84:320–41.

30. Vos de Wael R, Benkarim O, Paquola C, Lariviere S, Royer J, Tavakol S, et al. BrainSpace: a toolbox for the analysis of macroscale gradients in neuroimaging and connectomics datasets. Commun Biol. 2020;3(1):103.

31. Burt JB, Helmer M, Shinn M, Anticevic A, Murray JD. Generative modeling of brain maps with spatial autocorrelation. Neuroimage. 2020;220:117038.

32. Lariviere S, Royer J, Rodríguez-Cruces R, Paquola C, Caligiuri ME, Gambardella A, et al. Structural network alterations in focal and generalized epilepsy assessed in a worldwide ENIGMA study follow axes of epilepsy risk gene expression. Nat Commun. 2022;13(1):4320.

33. Lariviere S, Paquola C, Park B-y, Royer J, Wang Y, Benkarim O, et al. The ENIGMA toolbox: multiscale neural contextualization of multisite neuroimaging datasets. Nat Methods. 2021;18:698–700.

34. Chang CC, Lin CJ. LIBSVM: a library for support vector machines. ACM Trans Intell Syst Technol. 2011;2(3):1–27.

35. Shinn M, Hu A, Turner L, Noble S, Preller KH, Ji JL, et al. Spatial and temporal autocorrelation weave complexity in brain networks. *bioRxiv.* 2022.

36. Paquola C, Bethlehem RA, Seidlitz J, Wagstyl K, Romero-Garcia R, Whitaker KJ, et al. Shifts in myeloarchitecture characterise adolescent development of cortical gradients. Elife. 2019;8:8.

37. Zeng H, Pizarro R, Nair VA, La C, Prabhakaran V. Alterations in regional homogeneity of resting-state brain activity in mesial temporal lobe epilepsy. Epilepsia. 2013;54(4):658–66.

38. Meisel C. Antiepileptic drugs induce subcritical dynamics in human cortical networks. Proc Natl Acad Sci U S A. 2020;117(20):11118–25.

39. Girardi-Schappo M, Fadaie F, Lee HM, Caldairou B, Sziklas V, Crane J, et al. Altered communication dynamics reflect cognitive deficits in temporal lobe epilepsy. Epilepsia. 2021;62(4):1022–33.

40. Pitkänen A, Sutula TP. Is epilepsy a progressive disorder? Prospects for new therapeutic approaches in temporal-lobe epilepsy. Lancet Neurol. 2002;1(3):173–81.

41. Davis KA, Nanga RPR, Das S, Chen SH, Hadar PN, Pollard JR, et al. Glutamate imaging (GluCEST) lateralizes epileptic foci in nonlesional temporal lobe epilepsy. Sci Transl Med. 2015;7(309):309ra161.

42. Galovic M, van Dooren VQH, Postma T, Vos SB, Caciagli L, Borzi G, et al. Progressive cortical thinning in patients with focal epilepsy. JAMA Neurol. 2019;76(10):1230–9.

43. Akman CI, Ichise M, Olsavsky A, Tikofsky RS, Heertum RLV, Gilliam F. Epilepsy duration impacts on brain glucose metabolism in temporal lobe epilepsy: results of voxel-based mapping. Epilepsy Behav. 2010;17(3):373–80.

44. Kaestner E, Reyes A, Chen A, Rao J, Macari AC, Choi JY, et al. Atrophy and cognitive profiles in older adults with temporal lobe epilepsy are similar to mild cognitive impairment. Brain. 2021;144(1):236–50.

45. Tai XY, Koepp M, Duncan JS, Fox N, Thompson P, Baxendale S, et al. Hyperphosphorylated tau in patients with refractory epilepsy correlates with cognitive decline: a study of temporal lobe resections. Brain. 2016;139(9):2441–55.

46. Sisodiya SM, Whelan CD, Hatton SN, Huynh K, Altmann A, Ryten M, et al. The ENIGMA-epilepsy working group: mapping disease from large data sets. Hum Brain Mapp. 2022;43(1):113–28.

47. Gleichgerrcht E, Munsell BC, Alhusaini S, Alvim MKM, Bargalló N, Bender B, et al. Artificial intelligence for classification of temporal lobe epilepsy with ROI-level MRI data: a worldwide ENIGMA-epilepsy study. Neuroimage Clin. 2021;31:31102765.

48. Narasimhan S, Gonzalez HFJ, Johnson GW, Wills KE, Paulo DL, Morgan VL, et al. Functional connectivity between mesial temporal and default mode structures may help lateralize surgical temporal lobe epilepsy. J Neurosurg. 2022;137(6):1571–81.

SUPPORTING INFORMATION

Additional supporting information can be found online in the Supporting Information section at the end of this article.